Supporting Online Material for

Electron Cryomicroscopy of *E. coli* Reveals Filament Bundles Involved in Plasmid DNA Segregation

Jeanne Salje,* Benoit Zuber, Jan Löwe

*To whom correspondence should be addressed. E-mail: jsalje@mrc-lmb.cam.ac.uk

Published 18 December 2008 on *Science* Express
DOI: 10.1126/science.1164346

This PDF file includes:

Electron cryomicroscopy of *E. coli* reveals filament bundles involved in plasmid DNA segregation

Jeanne Salje, Benoît Zuber and Jan Löwe

SUPPORTING ONLINE MATERIAL

Materials and Methods

Plasmids and strains

ParM was expressed to high levels for purification and/or cryosectioning and tomography using plasmids pJSC1 (*1*) (wild type ParM, T7 promoter) or pRBJ212 (*2*) (D170A ParM, *ptac* promoter). The low-copy number R1-derived plasmid pKG491 (*3*) was used in vitreous sectioning and immunofluorescence microscopy experiments. Plasmid pJSC7 was constructed by introducing 3 copies of the ParMR*C* cluster from plasmid pDD19 (*4*) into a pUC19 derivative (pBR322 replicon) using PCR amplification and restriction cloning.

Wild-type ParM expression from pJSC1 used *E. coli* strain BL21-AI (Invitrogen) as host and D170A ParM was expressed from pRBJ212 in *E. coli* strain BR226. The *E. coli* K12 derivative CSH50 (*ara* Δ*(lac pro) thi rpsL*) was used for all experiments using pKG491 or pJSC7, and for imaging plasmid-free control cells.

Media and growth conditions

LB media was used in all experiments except for protein purification where cells were grown in 2xTY. Cells carrying pJSC1, pRBJ212 and pJSC7 were grown at 37 °C and those carrying pKG491 or no plasmid grown at 30 °C. All plasmids carried the *lacA* gene and ampicillin was used at 100 μg/mL. ParM expression from pJSC1 was induced using 0.2 % arabinose for 1-3 hours and D170A ParM expression from pRBJ212 was induced using 20 μM IPTG for 2 hours. A22 was diluted in methanol and added to growing cells at a final concentration of 10 μg/mL for 2 hours.

Protein purification

R1 ParM was purified as described previously (*5*).

In vitro crowding experiments

5 μM purified ParM was polymerized using 2 mM AMP-PNP in polymerization buffer (30 mM Tris-HCl, 100 mM KCl, 2 mM $MgCl_2$, pH7.5) in the presence or absence of 8 % PEG-6000. Samples were incubated at room temperature for 30 min. For negative strain electron microscopy, 4 μL of the reaction mixture was pipetted onto a glow-discharged carbon-coated grid and stained using 2 % uranyl acetate. For electron cryomicroscopy, the sample was placed on a glow-discharged holey carbon film (Quantifoil) and plunge frozen into liquid

ethane. Grids were transferred to and stored in liquid nitrogen.

Immuno blot

Cells were grown to mid-log phase and protein expression was induced where appropriate. Cells were mixed with SDS-PAGE loading buffer to an equivalent final cell concentration. Samples were run on SDS-PAGE gel, transferred onto a nitrocellulose membrane and incubated using affinity purified rabbit anti ParM primary antibody and HRP-conjugated secondary antibody. Immuno blots were developed using SuperSignal West Pico Chemiluminescent Substrate (Pierce).

Whole cell plunge freezing

BR226 cells carrying the pRBJ212 plasmid were induced with IPTG and grown to mid-exponential phase. 4 μL of cells were taken directly from the growth medium and mixed with 1 μL 10 nm gold-conjugated protein A. This was immediately placed on a glow-discharged holey carbon grid (Quantifoil, Cu/Rh 300 mesh, R3.5/1), and plunge frozen into liquid ethane. The grid was transferred to and stored in liquid nitrogen.

High pressure freezing and vitreous sectioning

Cells were grown to an OD_{600} of 0.5-0.7 (pJSC7, PKG491 or plasmid-free) or induced with arabinose and grown to OD_{600} ~1.0 (pJSC1). Cells in culture were centrifuged and re-suspended twice in PBS with 30% dextran (35-45 kDa). Samples were frozen in either copper tubes or caps and vitrified at 2000 bar using an EMPACT2 high-pressure freezer (Leica-Microsystems). Samples were mounted in the LEICA EM FC6 cryo-ultramicrotome (Leica Microsystems) operating at ñ140°C. A trimming knife (Diatome) was used to generate a pyramid and a 35° diamond knife (Diatome) used to cut sections. Ribbons prepared for standard transmission imaging were sectioned with a nominal feed of 50 nm, and placed on a carbon-coated 1000 mesh copper grid (Agar Scientific). Sections prepared for electron cryotomography were of a nominal feed of 150 nm and placed on carbon coated 400 x 100 mesh copper grids (Agar Scientific). Grids were stored in liquid nitrogen.

Electron microcopy

Negative stain electron microscopy was performed at 120 kV using a Tecnai 12 electron microscope operating at a pixel size of 0.24 to 0.42 nm. Electron cryomicroscopy imaging was performed at 300 kV either on an FEI F30 or an FEI Tecnai G2 Polara (FEI Company, Eindhoven, NL) at a pixel size of 0.56 to 0.67 nm. A22-treated cells and some plasmid-free cells were imaged on a helium-cooled JEOL microscope operating at 300 kV. Images for electron cryotomography were collected using an FEI Tecnai G2 Polara (300 kV, liquid nitrogen cooling, FEI company, Eindhoven, NL) equipped with a Gatan energy filter (filter bandpass 20 eV) on a 2 x 2 k Gatan Ultrascan CCD camera (plunge frozen samples) or a 4 x 4 k Gatan Ultrascan CCD

camera (vitreous sections) (Gatan, Pleasanton, CA). Tilt series were collected around a single axis at 1° or 2° increments between +/- 50° or 60° using either FEI Tomography Acquisition software (plunge frozen) or SerialEM acquisition software (vitreous sections) (*6*). The defocus was set at -12 μM for plunge frozen cells and -5 μM for tomography of vitreous sections. The cumulative dose was kept just low enough to prevent bubbling of the sample.

Image processing

Tomographic reconstructions were calculated using the IMOD tomography software package (*7*). 10 nm colloidal gold fiducial makers were used to align plunge-frozen samples, and fiducial-less alignment was used for vitreous sections. Magnifications were calibrated using catalase crystal diffraction patterns and fourier transform measurements were made using both ImageJ (*8*) and IMOD (*7*). Images were colored and annotated using Adobe Photoshop and Illustrator CS3. Images were manually cropped and subsequent manipulations were applied to the whole image. In figures S2-S4 a Gaussian blur with a 0.5 pixel radius and a high-pass filter with 25 pixel radius was applied to reduce noise. Images were then reduced to 8 bit grey scale resolution and compressed with JPEG.

Immunofluorescent microscopy

Cells were grown under exactly the same conditions as used for high pressure freezing and vitreous sectioning. Membranes were stained using 10 μg/mL FM-464 for ten minutes. 200 μL of cells were taken directly from cell culture, mixed with 1 mL ice-cold methanol and stored at – 20 °C for at least 2 hours. Slides were prepared as described previously (*9*) using affinity-purified rabbit anti-ParM antibodies at a 1:250 dilution and FITC-conjugated anti-rabbit (Sigma) at a 1:100 dilution. Cells were imaged using a Nikon Eclipse E800 microscope with Plan Apo 100x/1.40 oil DIC objective and a Photometrics CoolSnap HQ2 camera.

Figure Legends

Fig. S1 (A): Vitreous cryosections of cells over-expressing ParM to high concentrations (plasmid JSC1). Cells are filled with dense, semi-ordered bundles of ParM filaments.These are easily recognized in end-on views due to their high contrast compared with other cellular features. Scale bar = 100 nm. **(B):** Vitreous cryosections of cells over-expressing ParM to high concentrations, in the presence of the MreB-depolymerizing drug A22. This demonstrates that the filaments which we observe are not formed by the chromosomally-encoded bacterial actin, MreB. Filaments in this image are seen sideways rather than end-on. Scale bar = 100 nm.

Fig. S2 (A-C): Vitreous cryosections of cells carrying the high-copy ParMR*C* plasmid pJSC7. Small bundles (A) as well as bundles mixed with single filaments, arranged within and around the ribosome-free zone (nucleoid) can be observed (B, C). Scale bar = 100 nm.

Fig. S3 (A-G): Vitreous cryosections of cells carrying the R1 low-copy number plasmid pGK491. Images show small bundles of 3-5 ParM filaments which are thought to be actively segregating or holding small clusters of plasmid DNA. The filaments can be recognized by their dimensions and packing when compared with figures S1 and S2 and by the strong contrast generated by the filaments being oriented end-on. Scale bar = 100 nm.

Fig. S4 (A-F): Negative control cells where no obvious bundle-like features are visible. Scale bar = 100 nm.

Fig. S5. R1 low-copy number plasmid pGK491 filament bundles tend to arrange around the vicinity of the nucleoid. A and B (top) are the same image as S3C, C and D (bottom) are the same as S3F. For clarity, the region free of high-contrast features is colored in yellow. It is thought that this region occludes ribosomes and is the region occupied by genomic DNA, termed the nucloid. ParM filaments are colored in red, the cytosol is light blue. Scale bar = 100 nm.

References

1. J. Salje, J. Löwe, *EMBO J* (2008).
2. J. Møller-Jensen, R. B. Jensen, J. Löwe, K. Gerdes, *EMBO J* **21**, 3119 (2002).
3. K. Gerdes, S. Molin, *J Mol Biol* **190**, 269 (1986).
4. M. Dam, K. Gerdes, *J Mol Biol* **236**, 1289 (1994).
5. F. van den Ent, J. Møller-Jensen, L. A. Amos, K. Gerdes, J. Löwe, *EMBO J* **21**, 6935 (2002).
6. D. N. Mastronarde, *J Struct Biol* **152**, 36 (2005).
7. D. N. Mastronarde, *J Struct Biol* **120**, 343 (1997).
8. M. D. Abramoff, Magelhaes, P.J., Ram, S.J., *Biophotonics International* **11**, 36 (2004).
9. S. G. Addinall, E. Bi, J. Lutkenhaus, *J Bacteriol* **178**, 3877 (1996).

Figure S1 A. ParM over-expression (pJSC1)

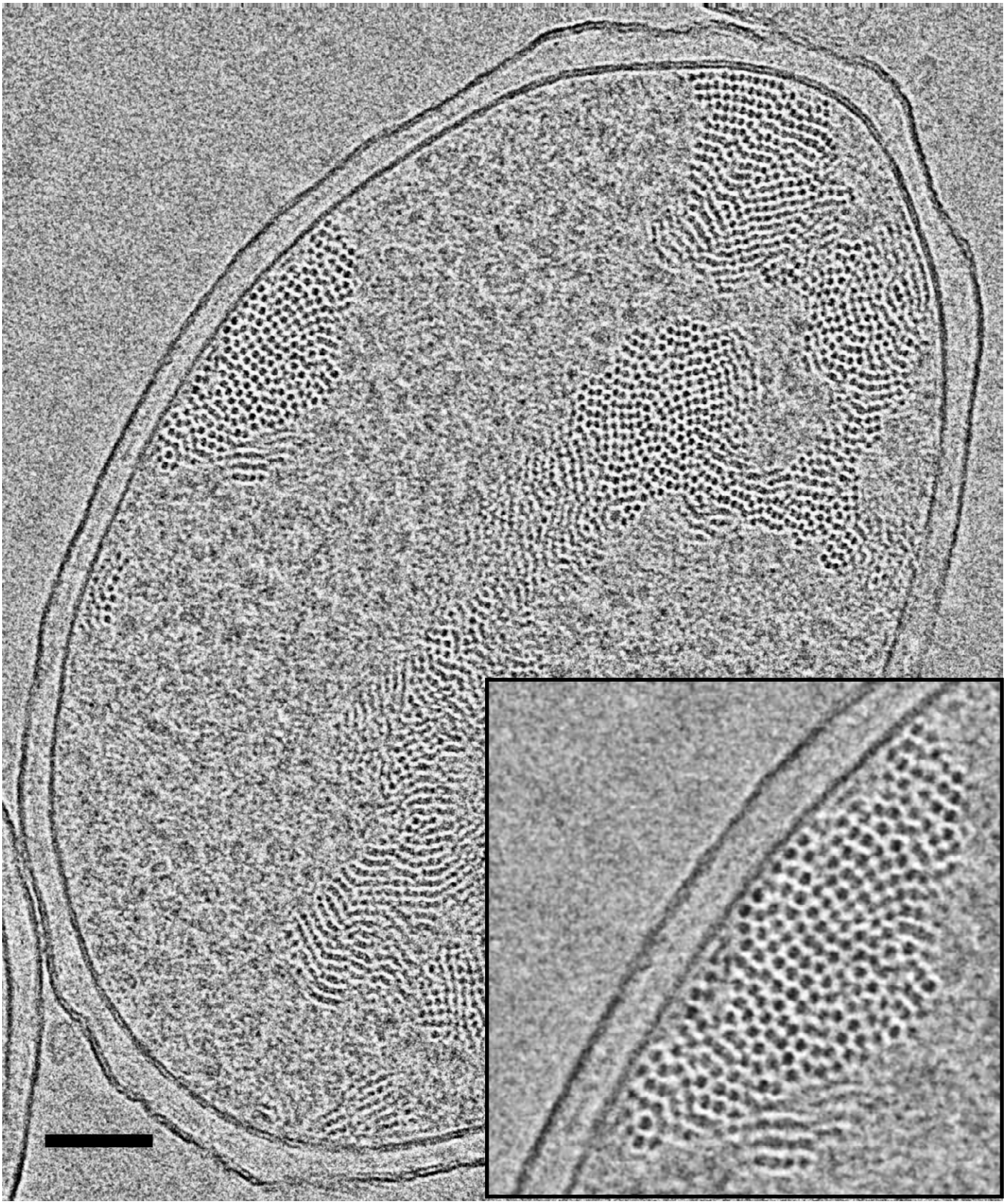

Figure S1 B. ParM over-expression (pJSC1), A22-treated

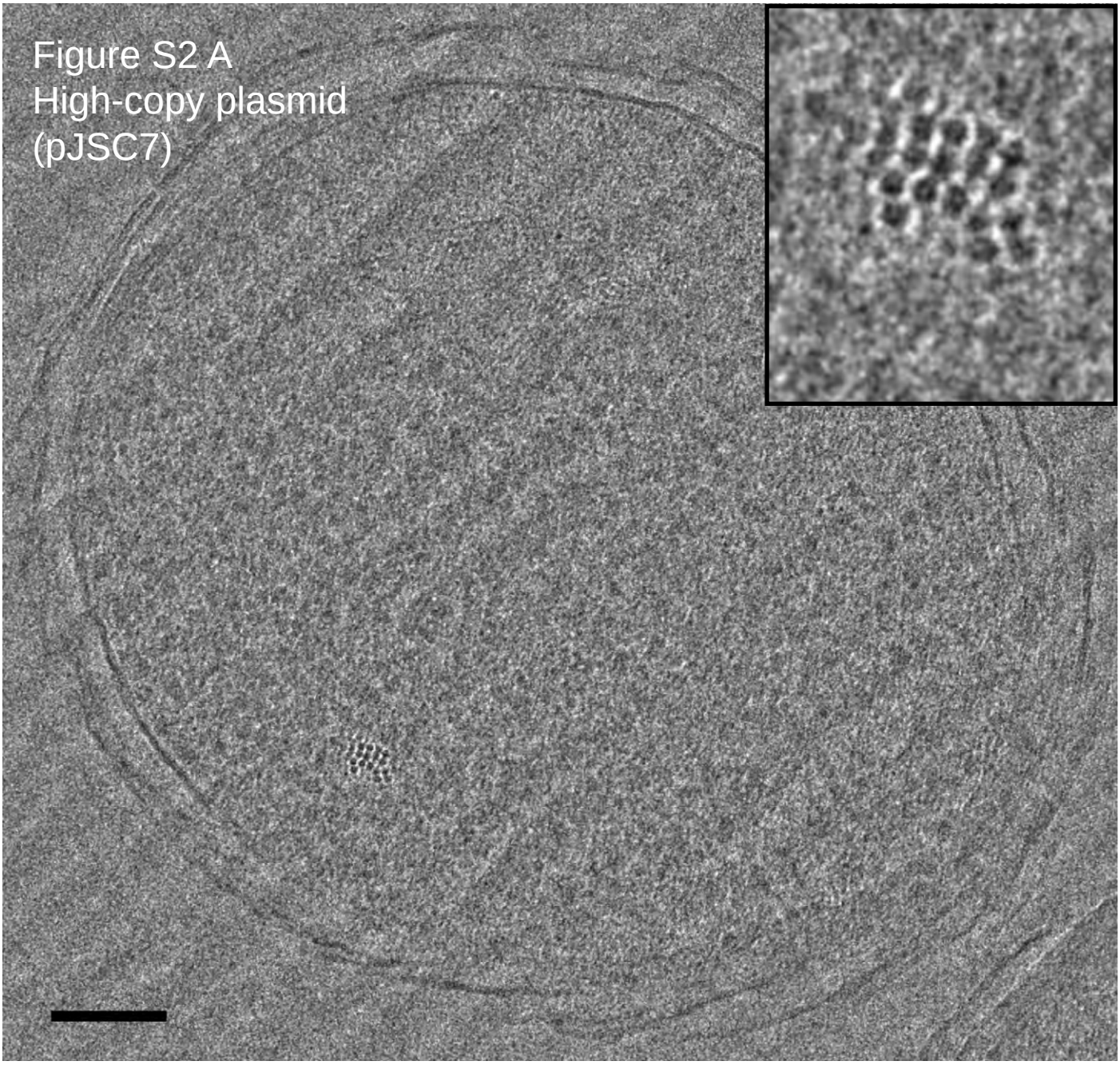
Figure S2 A
High-copy plasmid
(pJSC7)

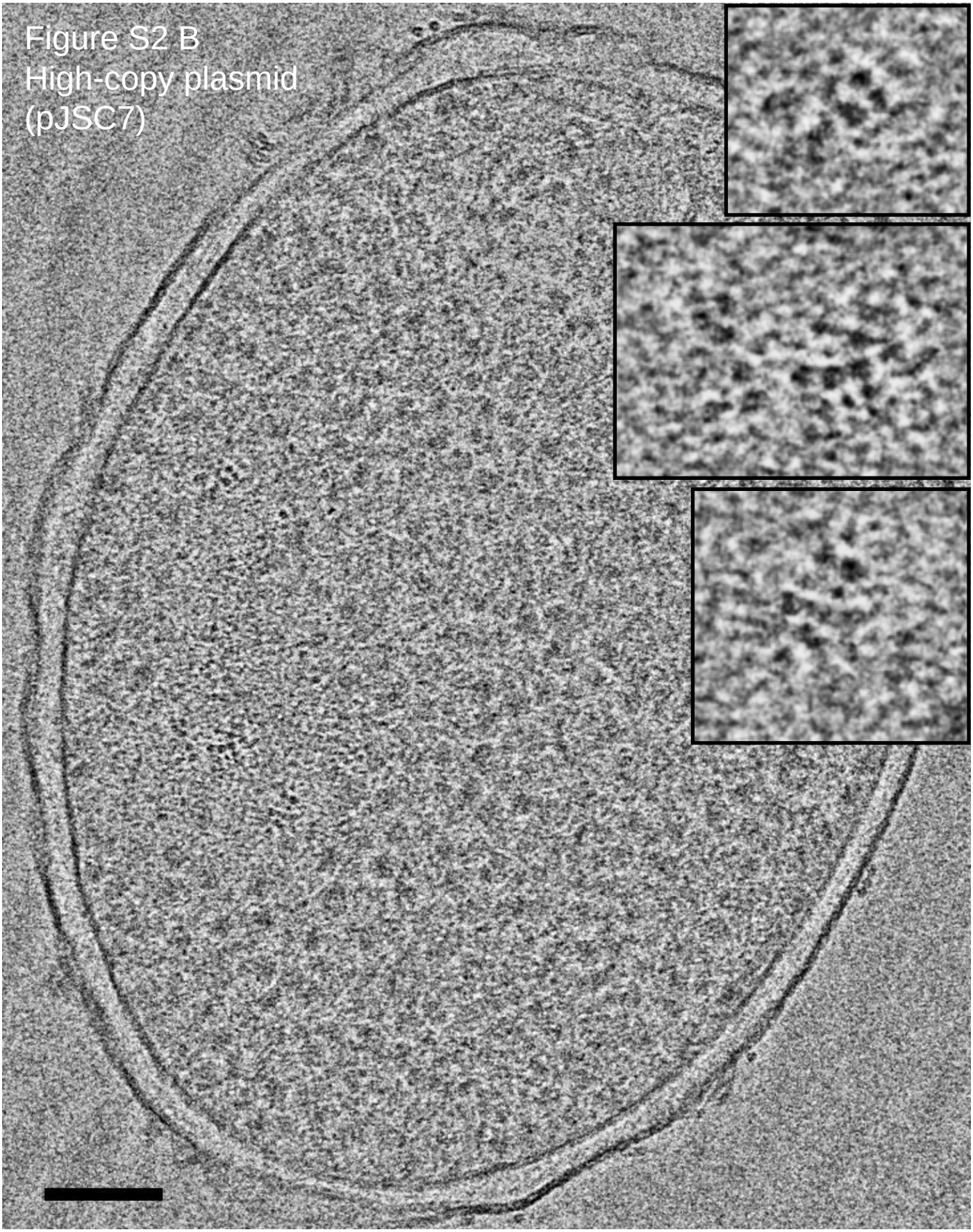
Figure S2 B
High-copy plasmid
(pJSC7)

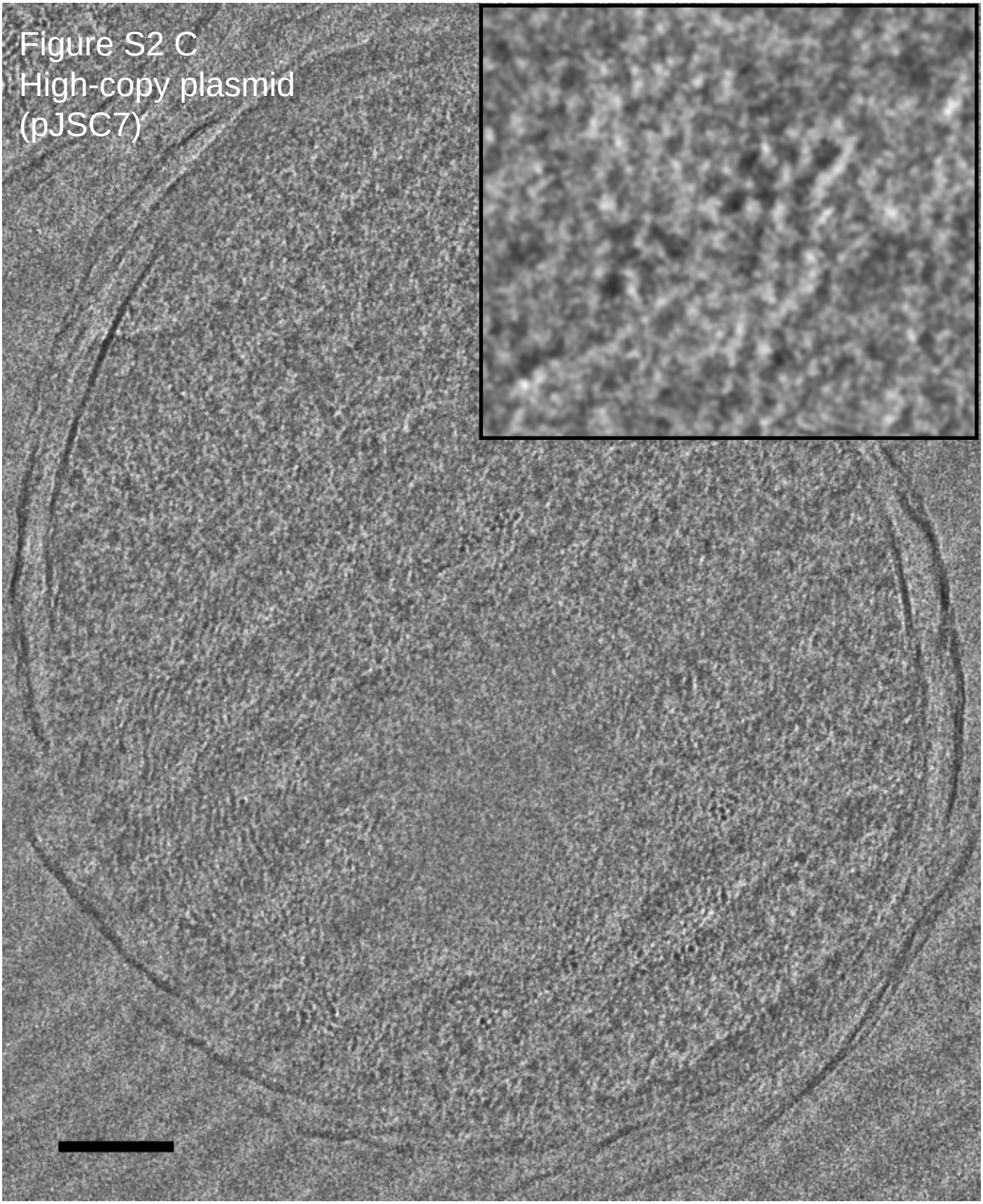
Figure S2 C
High-copy plasmid
(pJSC7)

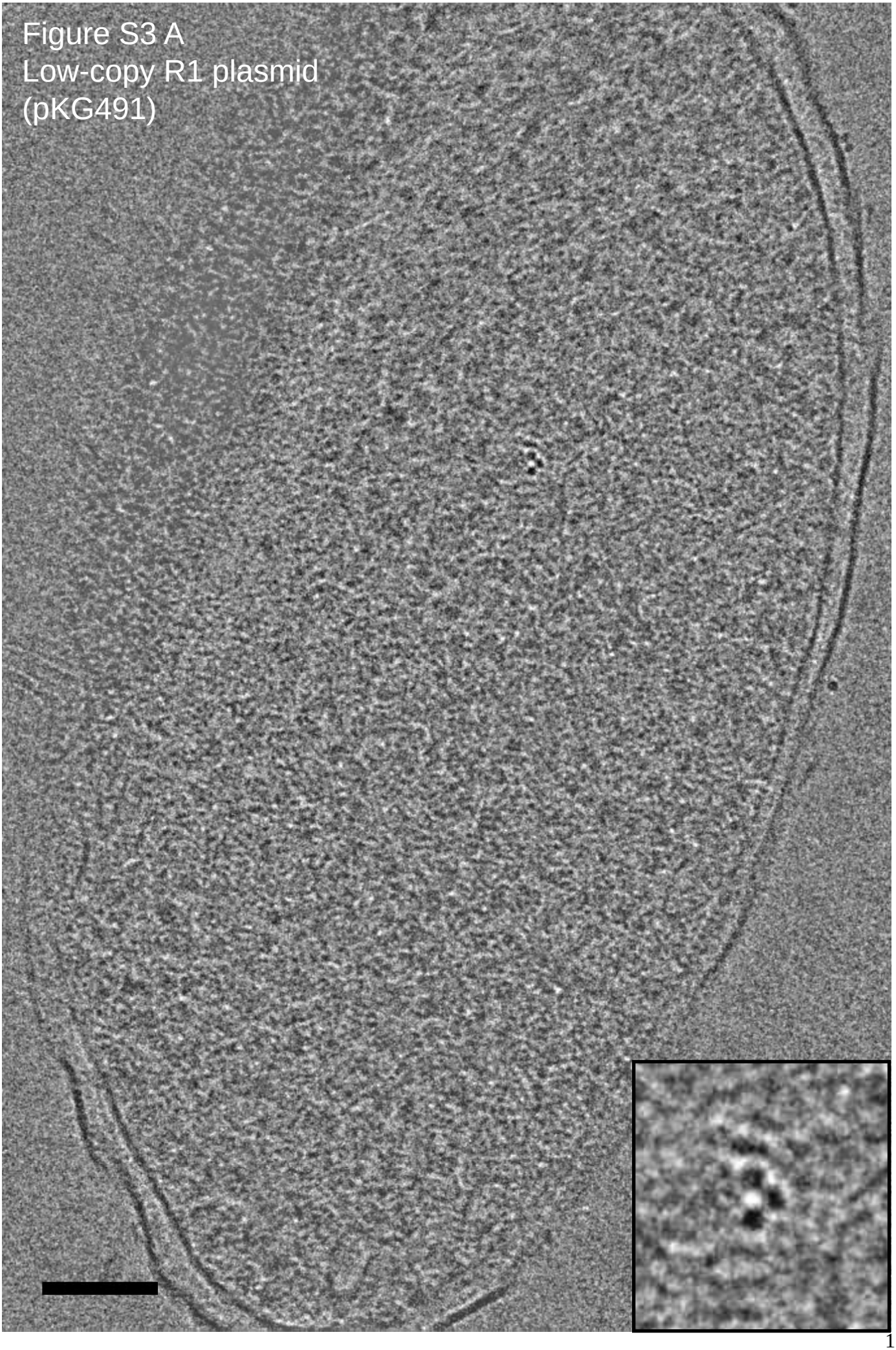
Figure S3 A
Low-copy R1 plasmid
(pKG491)

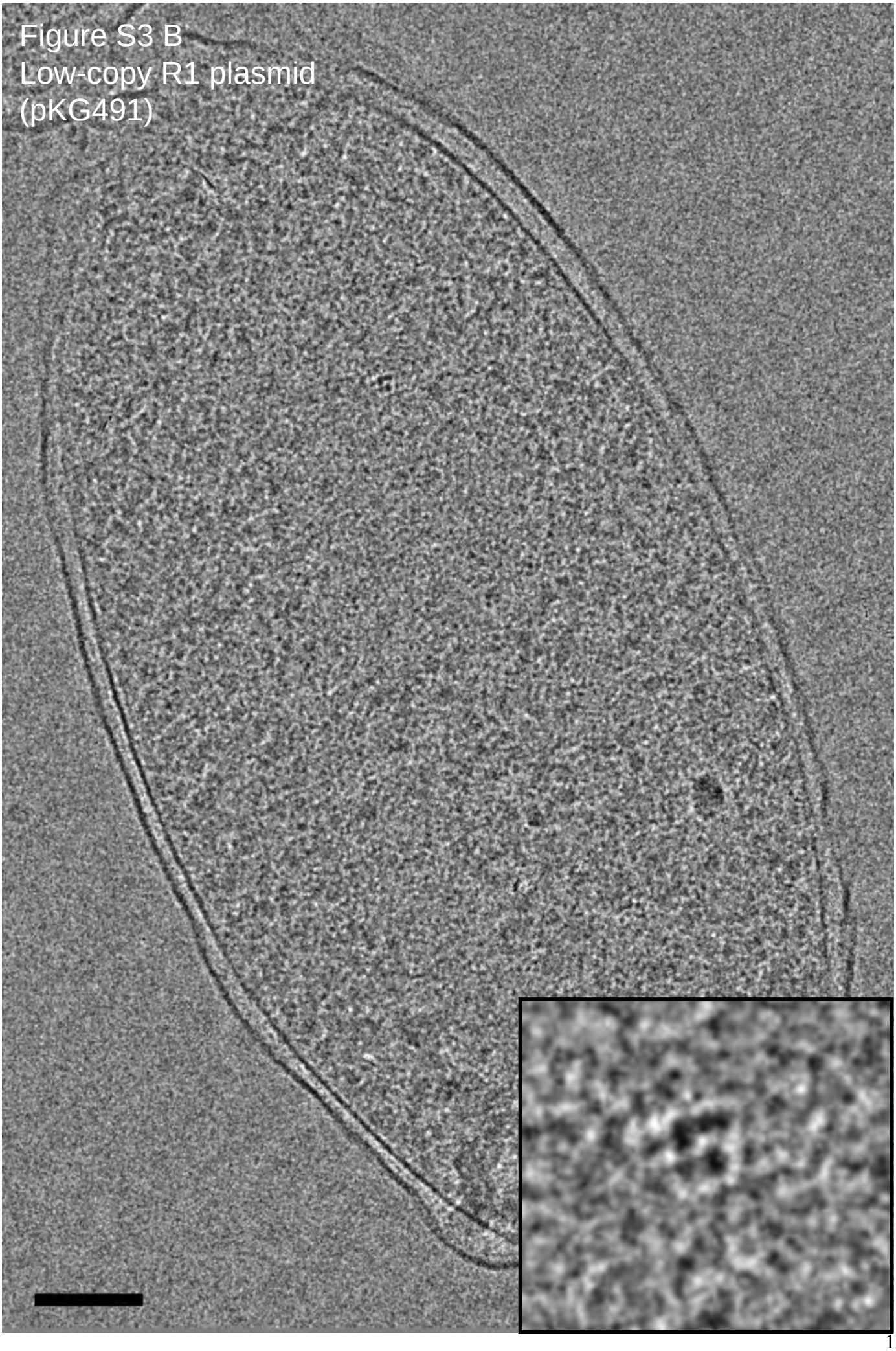
Figure S3 B
Low-copy R1 plasmid
(pKG491)

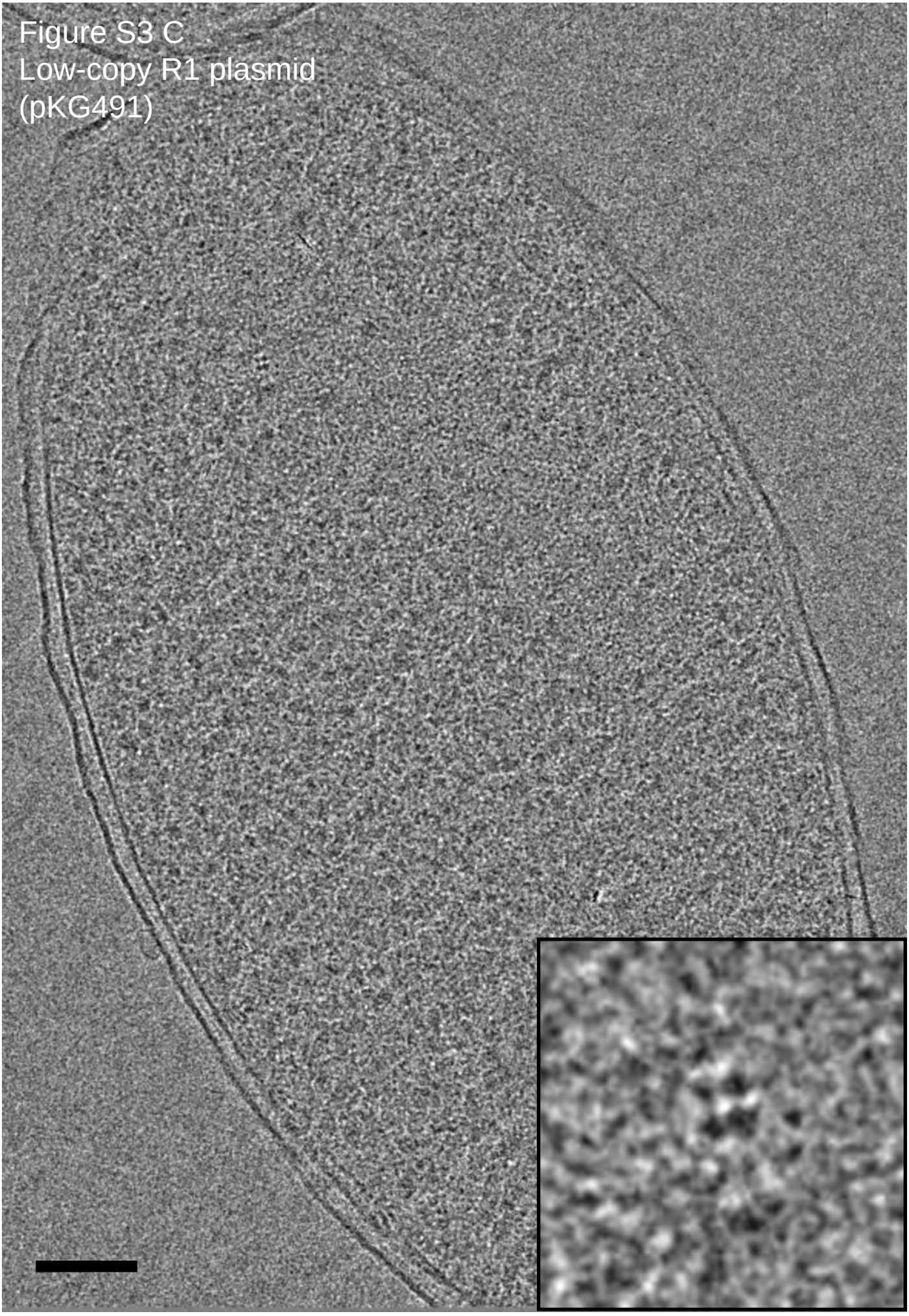
Figure S3 C
Low-copy R1 plasmid
(pKG491)

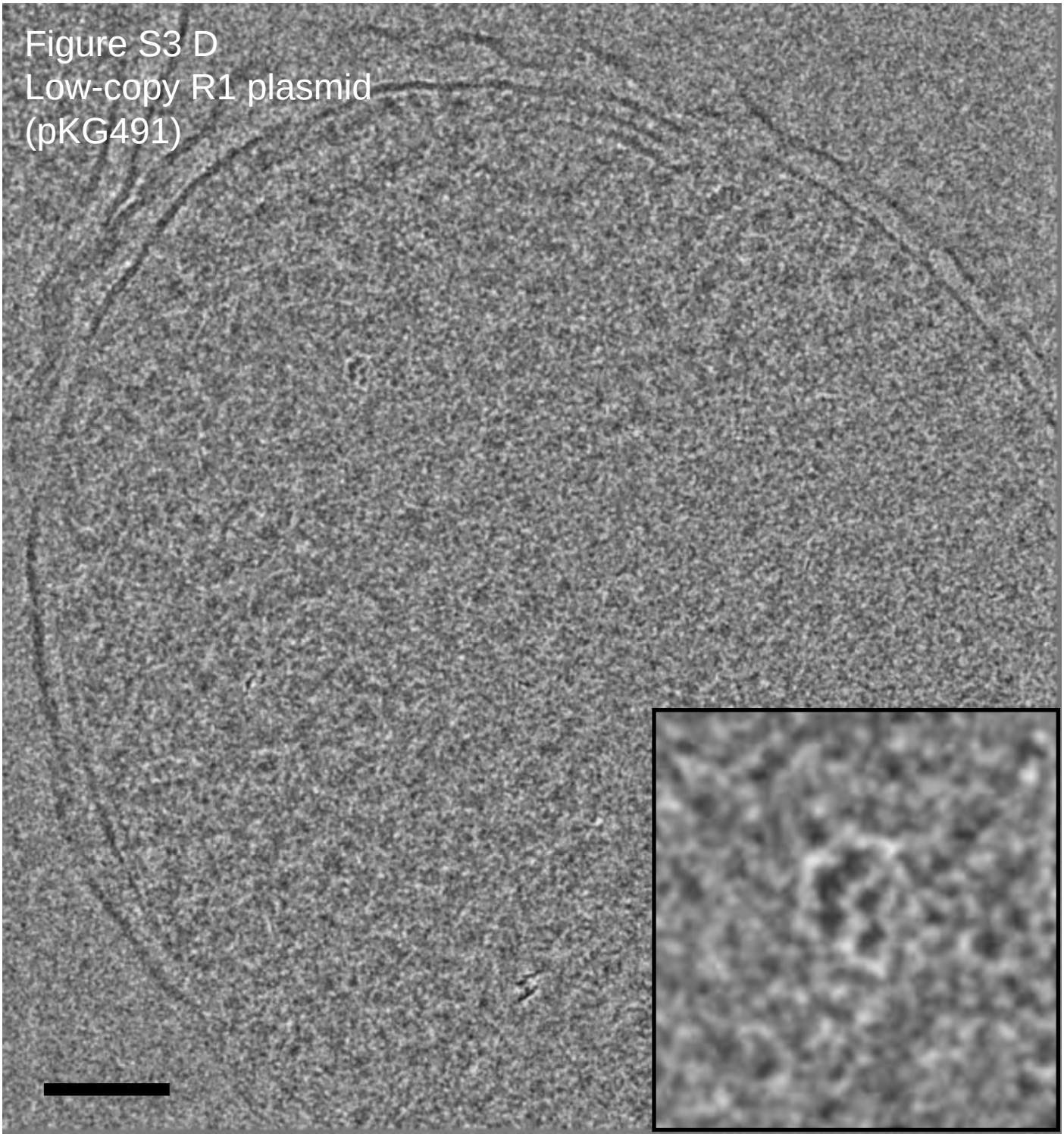
Figure S3 D
Low-copy R1 plasmid
(pKG491)

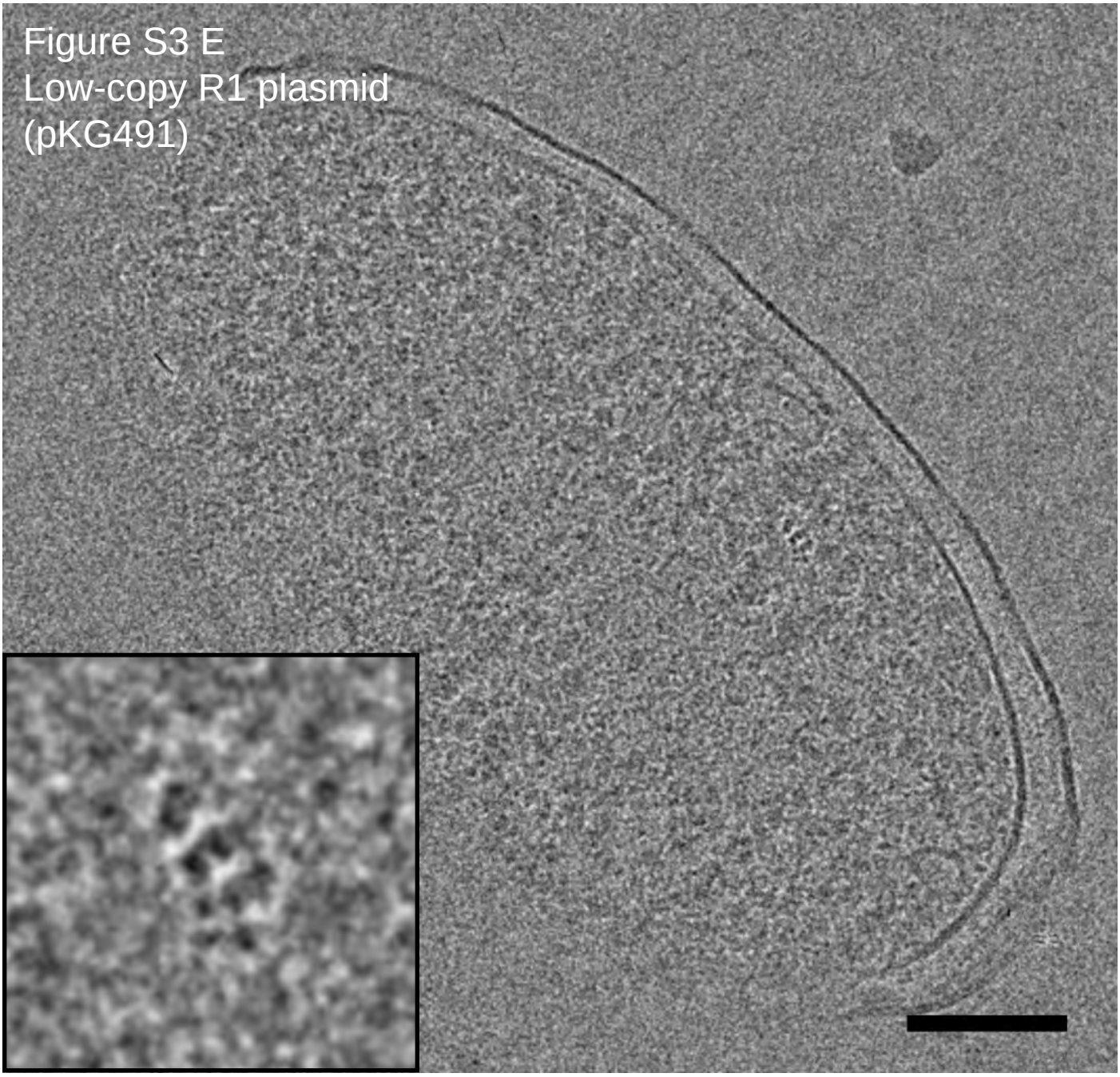
Figure S3 E
Low-copy R1 plasmid
(pKG491)

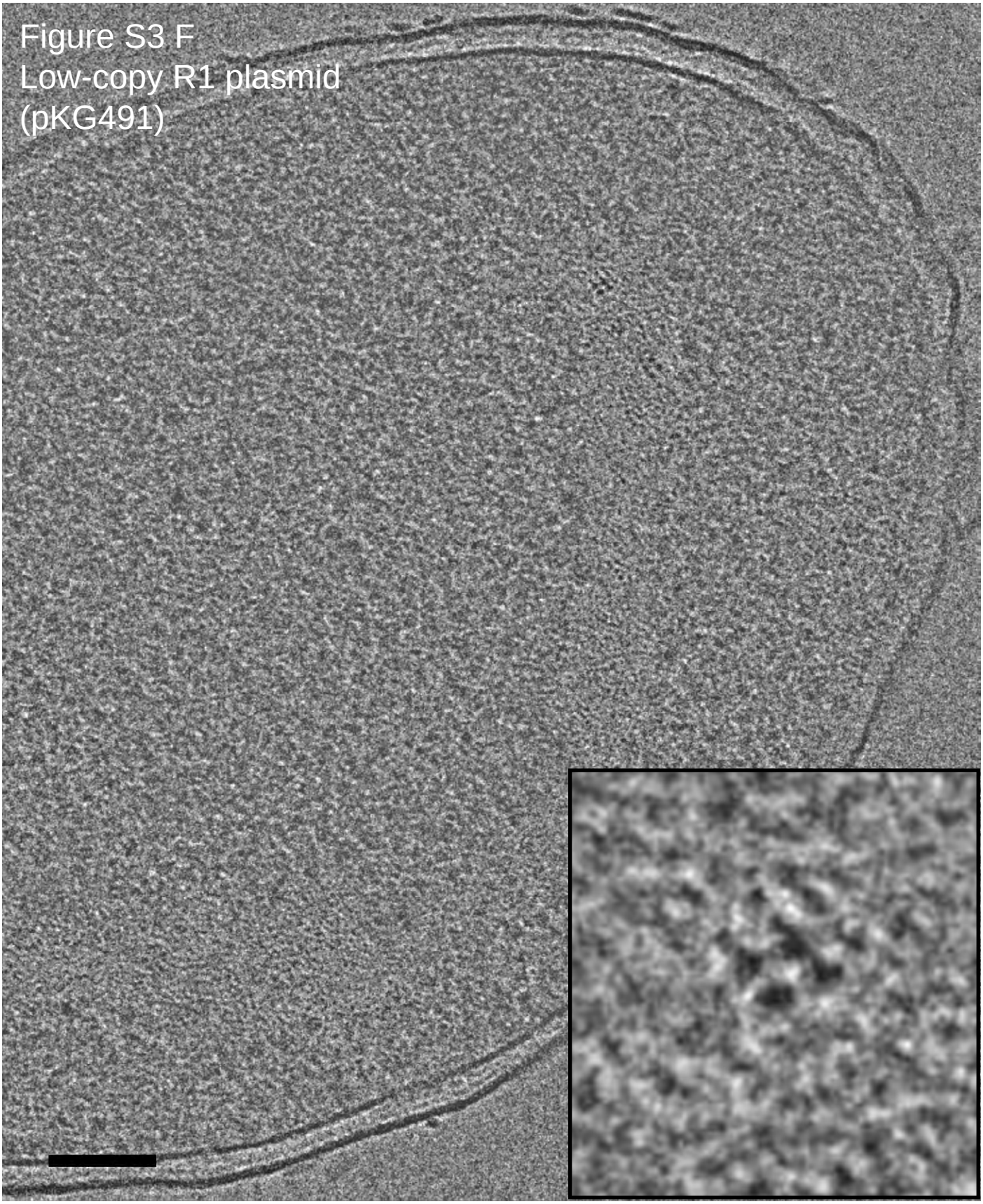
Figure S3 F
Low-copy R1 plasmid
(pKG491)

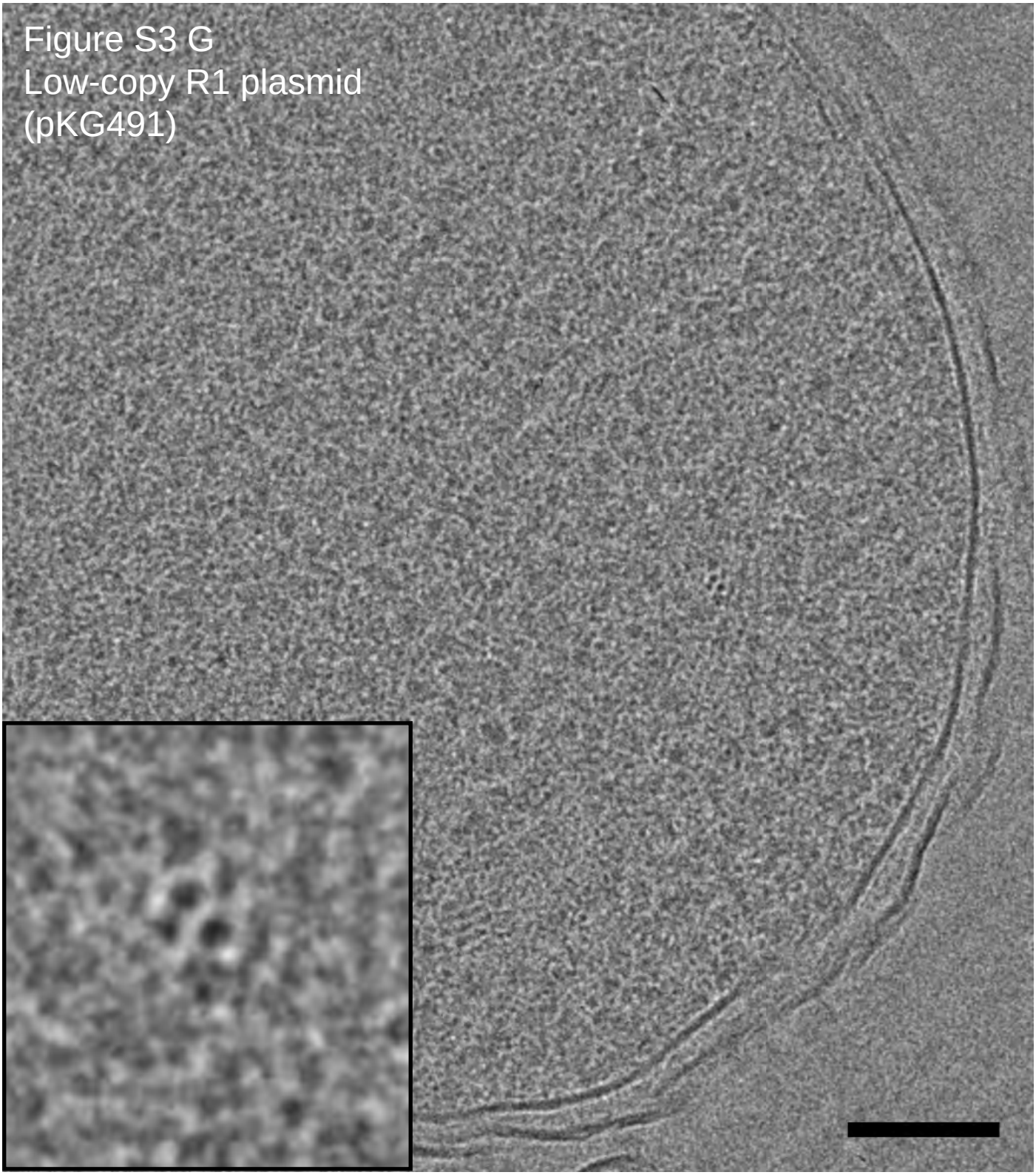
Figure S3 G
Low-copy R1 plasmid
(pKG491)

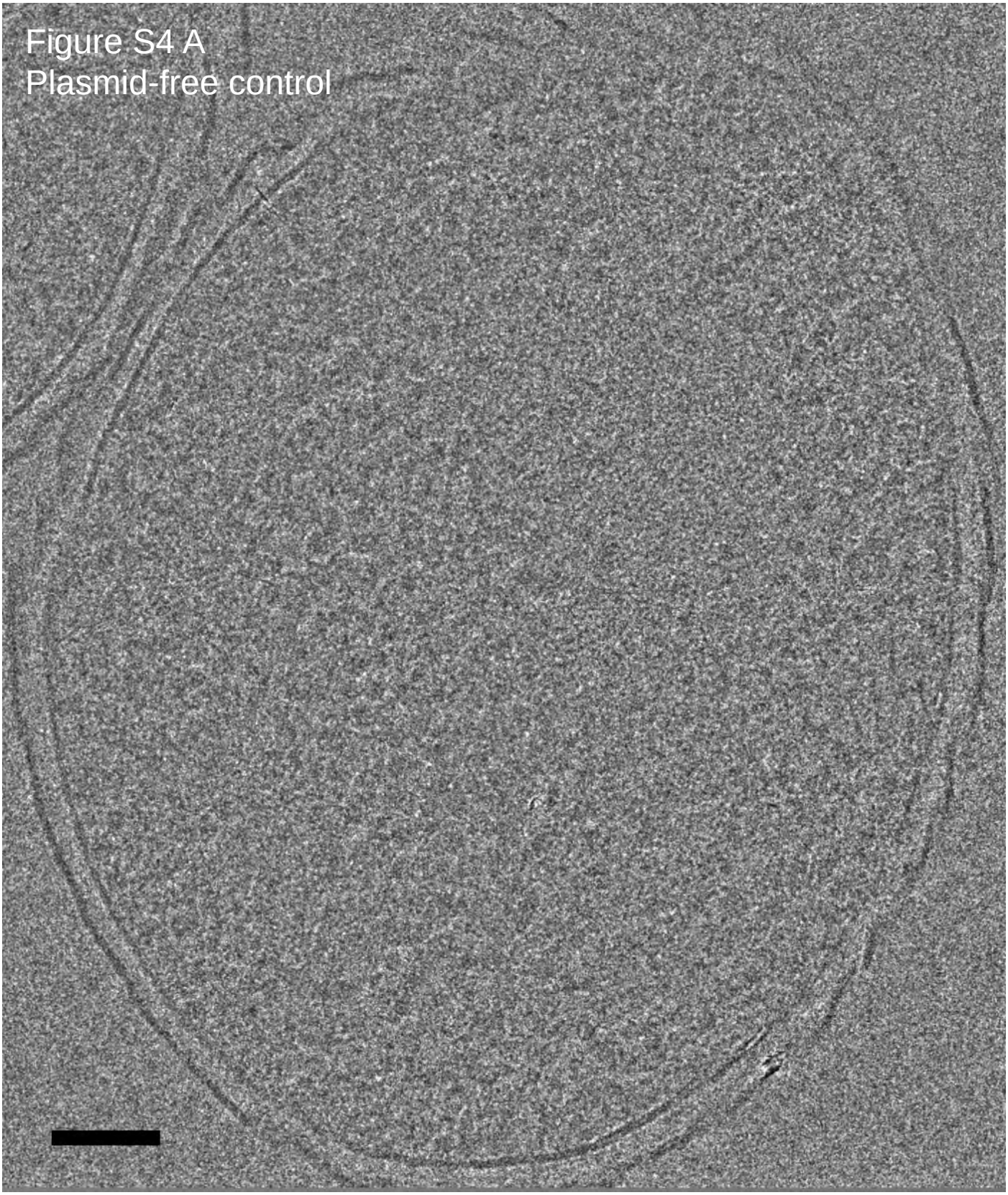
Figure S4 A
Plasmid-free control

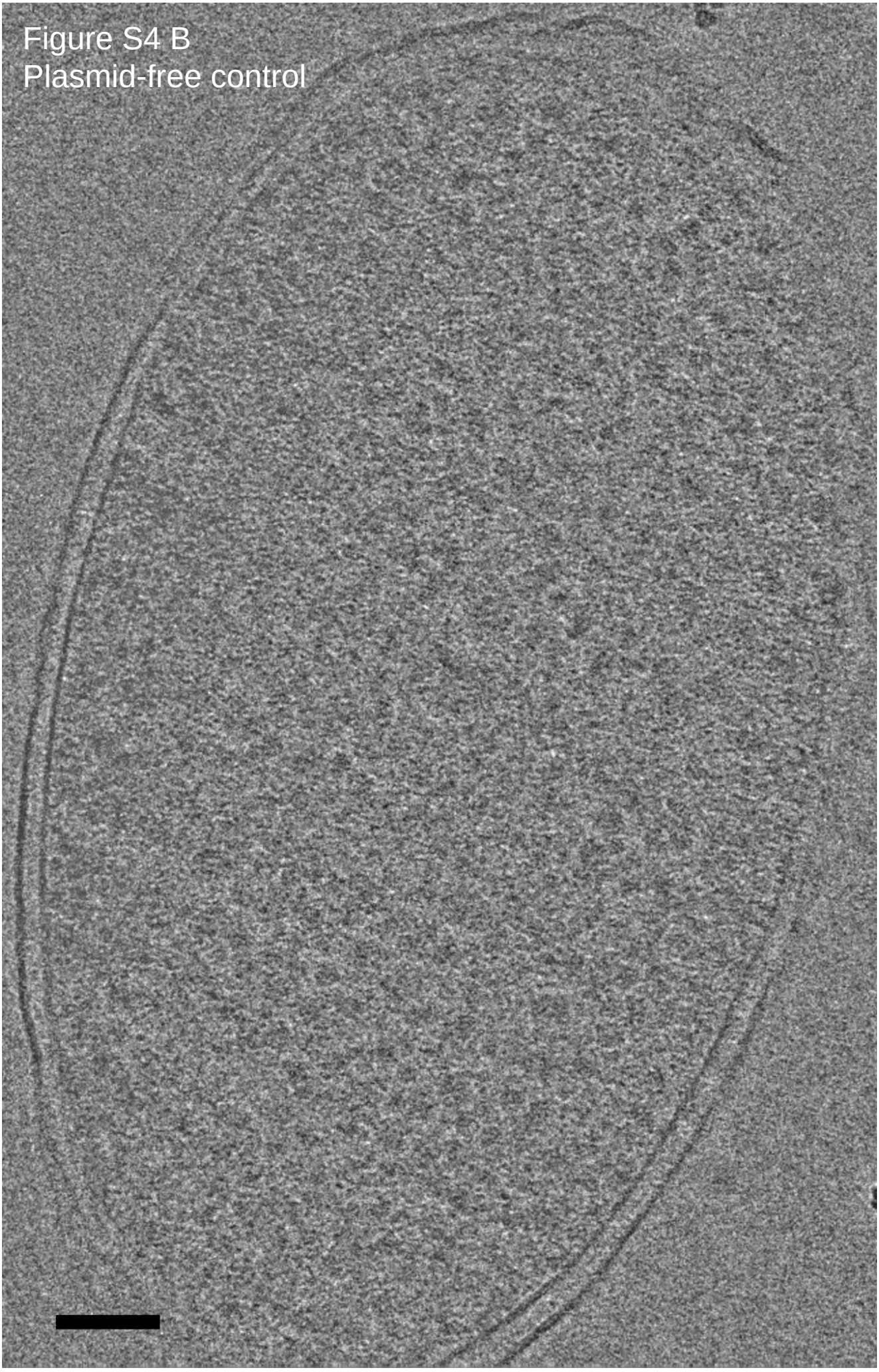
Figure S4 B
Plasmid-free control

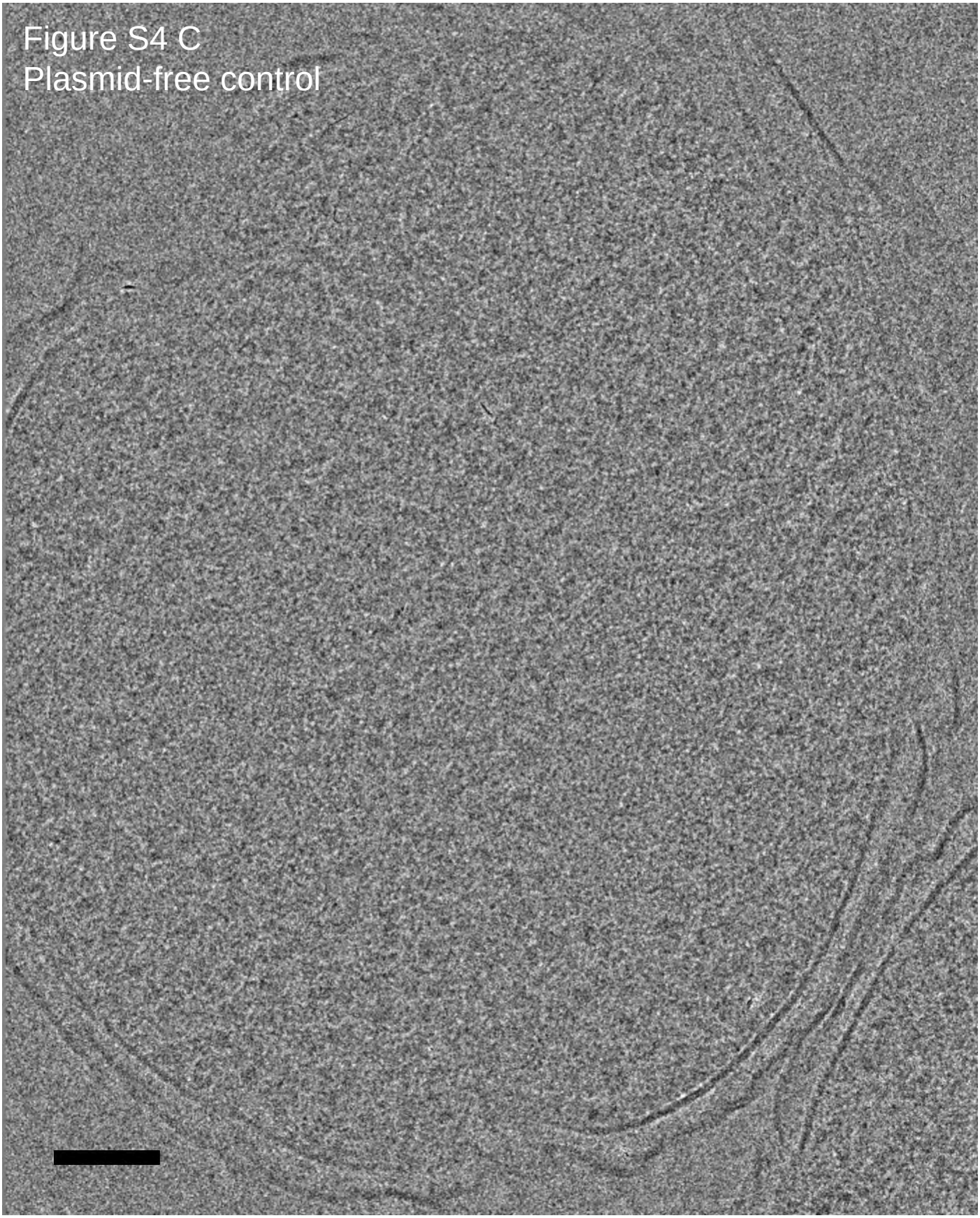
Figure S4 C
Plasmid-free control

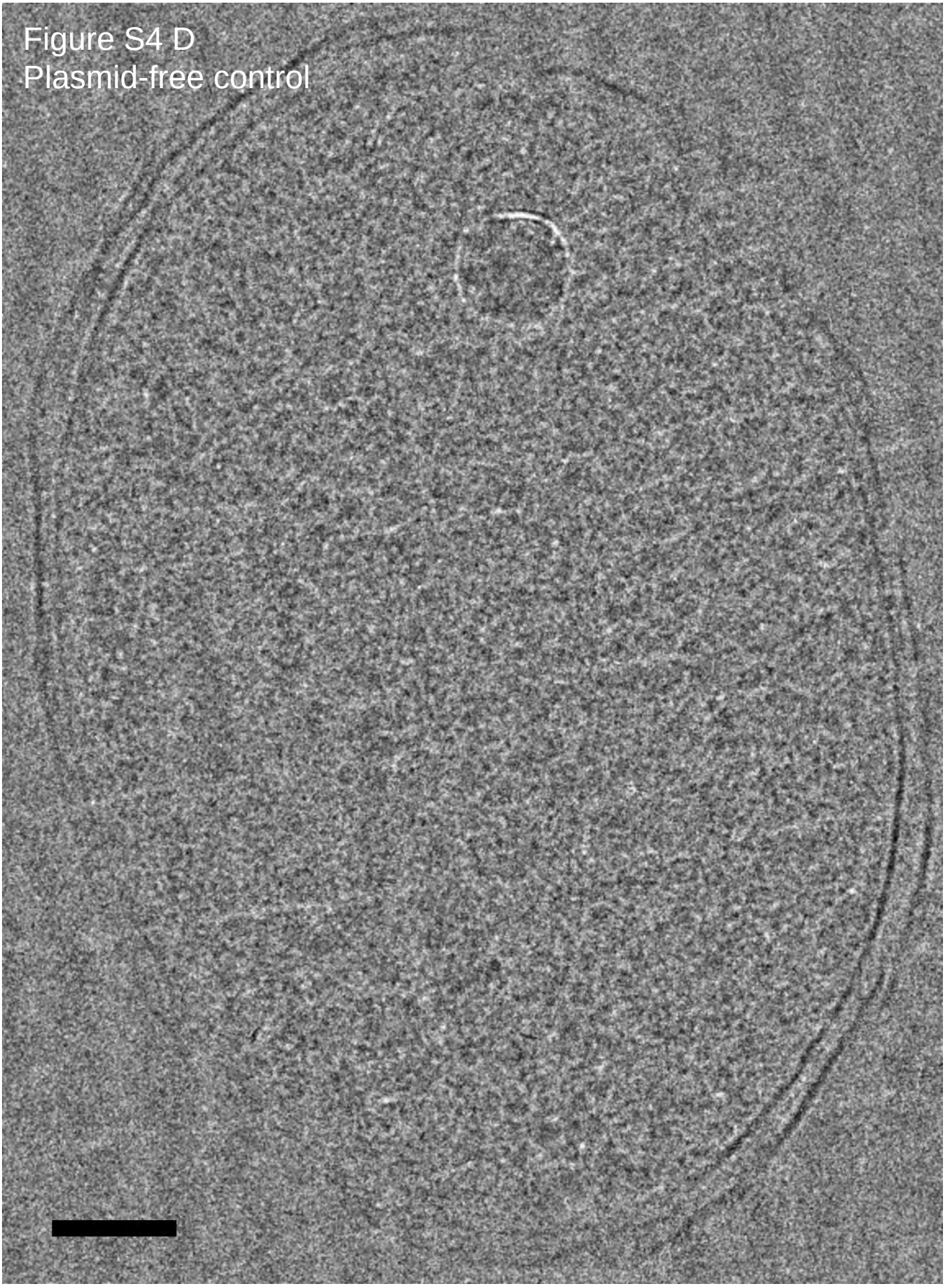
Figure S4 D
Plasmid-free control


Figure S4 E
Plasmid-free control

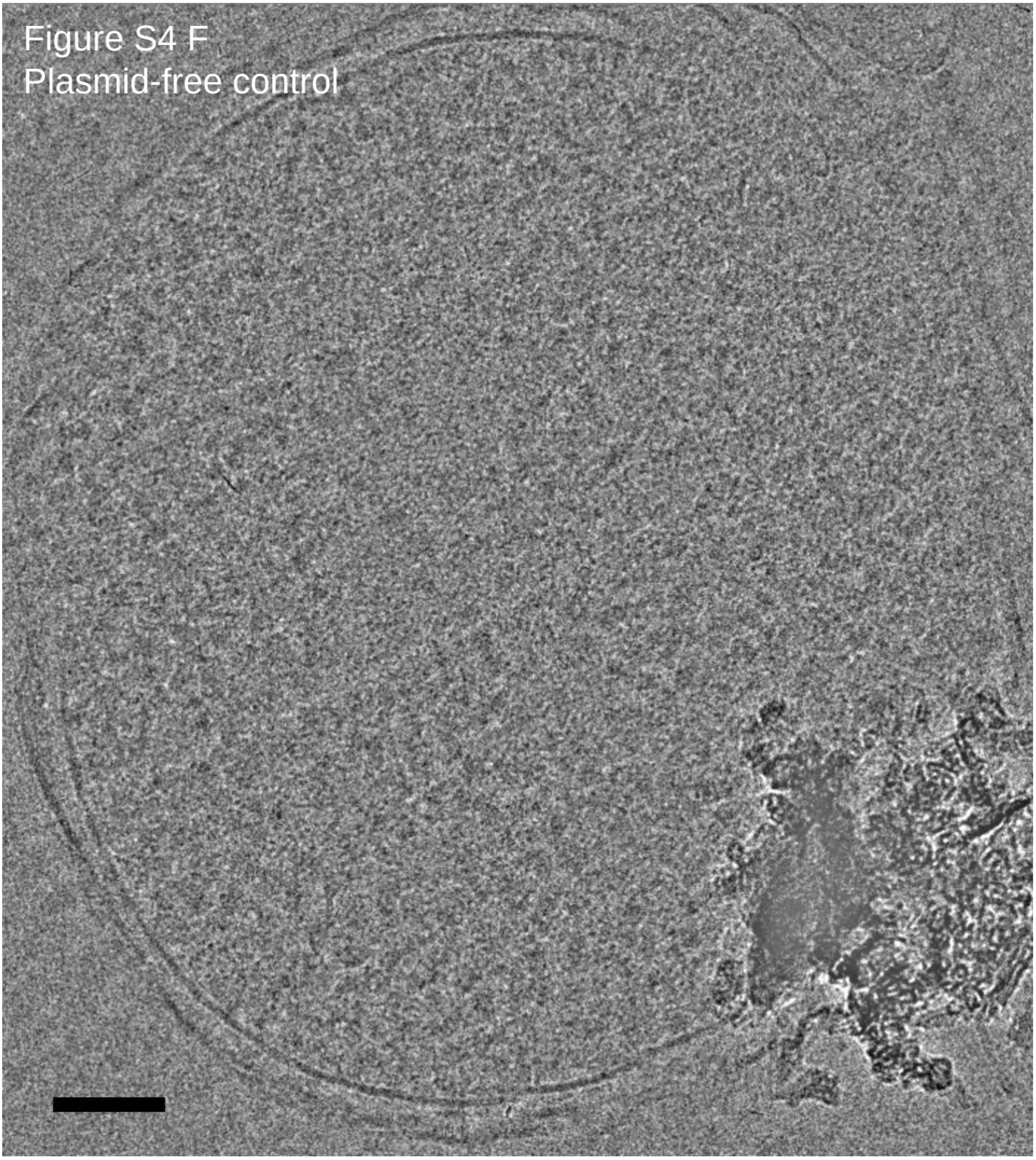
Figure S4 F
Plasmid-free control

Figure S5 low-copy number R1 plasmid (pKG491)